BNL-112555-2016-JA

Enhancing performance of PEM fuel cells: Using the Au nanoplatelet/Nafion interface to enable CO oxidation under ambient conditions

Hongfei Lia, Cheng Pan, Sijia Zhao,
Ping Liu, Yimei Zhu, Miriam H. Rafailovich

Submitted to Journal of Catalysis

July 2016

Chemistry Department

Brookhaven National Laboratory

U.S. Department of Energy
USDOE Office of Science (SC),
Basic Energy Sciences (BES) (SC-22)

Notice: This manuscript has been authored by employees of Brookhaven Science Associates, LLC under Contract No. DE- SC0012704 with the U.S. Department of Energy. The publisher by accepting the manuscript for publication acknowledges that the United States Government retains a non-exclusive, paid-up, irrevocable, world-wide license to publish or reproduce the published form of this manuscript, or allow others to do so, for United States Government purposes.

DISCLAIMER

This report was prepared as an account of work sponsored by an agency of the United States Government. Neither the United States Government nor any agency thereof, nor any of their employees, nor any of their contractors, subcontractors, or their employees, makes any warranty, express or implied, or assumes any legal liability or responsibility for the accuracy, completeness, or any third party's use or the results of such use of any information, apparatus, product, or process disclosed, or represents that its use would not infringe privately owned rights. Reference herein to any specific commercial product, process, or service by trade name, trademark, manufacturer, or otherwise, does not necessarily constitute or imply its endorsement, recommendation, or favoring by the United States Government or any agency thereof or its contractors or subcontractors. The views and opinions of authors expressed herein do not necessarily state or reflect those of the United States Government or any agency thereof.

Enhancing performance of PEM fuel cells: Using the Au nanoplatelet/Nafion interface to enable CO oxidation under ambient conditions

Hongfei Li[a,1], Cheng Pan[a], Sijia Zhao[a], Ping Liu[b], Yimei Zhu[c], Miriam H. Rafailovich[a,]

[a]*Department of Materials Science and Engineering, State University of New York at Stony Brook, Stony Brook, New York 11794, United States*
[b]*Department of Chemistry, Brookhaven National Laboratory, Upton, New York 11973, United States*
[c]*Department of Condensed Matter Physics and Materials Science, Brookhaven National Laboratory, Upton, New York 11973, United States*

Abstract

We have developed a method for fabrication of Au nanoparticle platelets which can be coated onto the Nafion membranes of polymer electrolyte membrane(PEM) fuel cells simply by Langmuir-Blodgett(LB) trough lift off from the air water interface. Incorporating the coated membranes into fuel cells with one membrane electrode assembly(MEA) enhanced the maximum power output by more than 50% when operated under ambient conditions. An enhancement of more than 200% was observed when 0.1% CO was incorporated into the H_2 input gas stream and minimal enhancement was observed when the PEM fuel cell was operated with 100% O_2 gas at the cathode, or when particles were deposited on the electrodes. Density function theory(DFT) calculations were carried out to understand the origin of improved output power. Au NPs with 3-atomic layer in height and 2 nm in size were constructed to model the experimentally synthesized Au NPs. The results indicated that the Au NPs interacted synergistically with the SO_3 groups, attached at end of Nafion side chains, to reduce the energy barrier for the oxidation of CO occurring at the perimeter of the Au NPs, from 1.292 eV to 0.518 eV, enabling the reaction to occur at T<300 K.

Keywords: PEM Fuel Cell, Gold Nanoplatelets, CO Oxidation

1. Introduction

Polymer electrolyte membrane membrane fuel cells (PEMFC) are an attractive source of energy because of their high power density[1], low operation temperature[2] and almost pollution-free emission[3]. In fuel cells, power is generated via the conduction of H^+ ions through a polyelectrolyte membrane, commonly composed of sulfonated tetrafluoroethylene based fluoropolymer-copolymer (Nafion). The function of the fuel cell constitutes a balance between hydrogen oxidation and oxygen reduction reactions where Pt nanoparticles are used to catalyze the reactions at the electrodes[4]. Under ambient conditions where CO_2 is present, CO is one of the byproducts of the fuel cell operation which is produced on the nafion membrane, as a result of the Pt catalyzed H_2 reduction at the anode, or via the reverse water gas shift reaction (RWGS) at the cathode[5]. In either case, the rate constant for oxidation of CO is lower than that for the other reactions, especially below 400 K, resulting in accumulation and subsequent migration to the electrodes where amounts, as low as 75 ppm, poison the Pt catalyst and can reduce the power output by more than 50%[6, 7].

Haruta *et al.*[8], Yates *et al.*[9] as well as several other groups[10, 11, 12] over the last decade have demonstrated that Au nanoparticles are very effective catalysts of the CO oxidation. An essential conditions of this process though was the formation of nanoplatelets with no more than three atomic layers thickness in direct contact with metal oxide supports, where a two-step catalytic process was postulated at the perimeter of the particles which reduced the energy barrier and increased the reaction rate[13, 14]. We have developed a robust method to produce hemispherical particles 2.71±0.83 nm in diameter and 1.7 nm thick, which do not need require a metal oxide support. The platelets are formed using the Langmuir method the air/water interface and are deposited as a uniform film directly on the nafion membranes. Hence, the polymer electrolyte membrane repalces the metal oxide as the moderator of the Au catalytic reaction. Here we show that the coated membranes can enhance the current and power output of

Email address: miriam.rafailovich@stonybrook.edu (Miriam H. Rafailovich)

[1]H.L. and C.P. contributed equally to this work.

PEMFCs, operated under ambient conditions, by more than 50%, without a corresponding increase in voltage. DFT calculations indicated that the particles, working in synergy with the SO_3 functional groups on the Nafion membrane reduced the activation barrier and increased the reaction rate constant for CO oxidation which was the rate limiting step at room temperature. The calculations indicated that the Nafion membrane participated in the two step catalysis process of the reverse gas shift reaction in the same manner as previously reported by Neurock and Yates[9] only for Au deposited on metal oxides. Haruta *et al.*[15] first demonstrated that Au nanoparticles could be effective catalysts of the CO oxidation at low temperatures when good contact with certain metal oxides (i.e.TiO_2) substrates is established. Neurock and Yates[16] proposed an explanation for this effect by assuming that the Au nanoparticles were oblate shaped and formed a stepped interface at the contact line with the TiO_2 substrate. The atomic steps then provided perimeter sites for adsorption of the reactants which enabled a two-step oxidation process to occur. In this model the substrate first interacted with the reactants, allowing bond stretching on the support surface. This decreased the barrier to the catalytic process which occurred on active sites at the perimeter of the Au nanoparticles thereby greatly increasing the efficiency and reducing the operating temperature of the CO oxidation[16, 17]. The model was not unique to Au NPs physcially deposited on TiO_2 substrate and a similar mechanism has been reported for Au NPs synthesized on other kinds of metal oxide supportors[18] by different methods[19]. Even though Haruta and others speculated that this type of reaction may also provide a solution for eliminating CO poisoning of PEM fuel cells, the metal oxide subsrate involved in formation and deposition of the particles were not practical for ion transportation, and hence incorporation into PEM fuel cells was never attempted.

We had previously developed a technique whereby

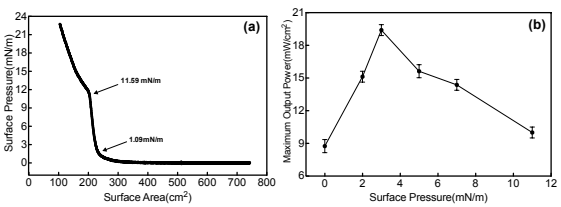

Figure 1: (a) π-A isotherms of as-prepared gold nanoparticles recording by Langmuir-Blodgett trough. (b) Coating surface pressure dependence for output power density of PEM fuel cell.

oblate shaped Au particle nanoplatelets, with an aspect ratio of approximately 2 and only three atomic layers thick, could be reproducibly formed at the air water interface, and then coated as a film onto any arbitrary surface simply by using the Langmuir-Blodgett technique[20]. Here we show that when this film is deposited directly onto the membrane of a PEM fuel cell, the efficiency of the cell is enhanced by more than 50%, when operated under ambient conditions.

Furthermore we show that this enhancement occurs only when the particles are placed as a single layer, in direct surface contact with the Nafion membrane, in a manner similar to the complexes reported on TiO_2. We therefore proposed that the two step catalysis process also occurs on the Nafion membrane, where the oxidation of CO at the perimeter of the Au nanoparticles is facilitated by the sulfonic groups present on the Nafion polymer. These results are consistent with DFT calculation which show that activation barrier for CO oxidation by the gold-sulfonic group complex temperature is reduced to 0.518 eV, enabling the reaction to occur at room temperature.

2. Materials and Methods

2.1. Fuel Cell Stacks

The tests described here were conducted using a 16 cm^2 single stack H-TEC EDUCATION, GmbH (Luebeck, Germany) F107 Demonstration PEMFC kit, with a specified maximum power output at room temperature of 200mW. The MEA for this cell consisted of a Nafion 117 membrane (Fuel Cell Etc., Texas, USA) sandwiched between 16 cm^2 electrodes at a Pt loading of 0.1mg/cm^2 (Fuel Cell Etc., Texas USA). The membrane was hydrated by immersion into DI water for at least five minutes before assembly. The MEA was press fit together with uniform pressure applied to a four-point screw assembly. The fuel cell test was accomplished using a test station assembled in our laboratory. A voltmeter (Flow 2076209 digital multimeter) and an ampere meter (Keithley 195A digital multimeter) were used to record the performance data. The load on the cell was applied across a precision resistance bridge (Resistance decade box 1171), which as varied manually. The gas flow rate was controlled by an analogue flow meter (Supelco) which was calibrated relative to a digital flow meter (Restek Proflow 6000) and used to monitor the gas flow speed.

2.2. Computational Method

The unrestricted DFT calculations were performed using the $DMol^3$ code[21, 22]. The ionic cores were

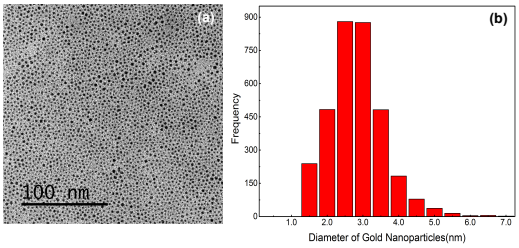

Figure 2: (a) Transmission electron microscopy(TEM) images and (b) core size distribution histogram of gold nanoparticles. The average core size is 2.71 nm.

described by effective core potentials (ECP). A numerical basis set was used with comparable accuracy to a Gaussian 6-31G (d) basis set. A local basis cutoff of 5.0 Å in real space was employed. The generalized gradient approximation (GGA) with PW91 functional[23] was utilized. The transition state (TS) was located by synchronous transit methods[24]. The Linear Synchronous Transit (LST) was conducted to bracket the maximum between the reactants and products, followed by repeated conjugate gradient minimizations and the Quadratic Synchronous Transit (QST) maximizations until a transition state was located. The convergence thresholds were set as that the root mean square (rms) forces on the atoms were smaller than 0.002 Ha/Å . Such methods yield results close to those obtained by eigenvector following methods. Au NPs were allowed to fully relax together with adsorbates with no constrain.

3. Results and Discussions

Thiol functionalized gold nanoparticles (Au NPs) were synthesized via the two-phase method developed by Brust *et al.*[25]. A 1 mg/ml Au NPs/toluene solution was prepared and 200μL were spread onto the surface of water by a glass syringe. The π-A isotherms of the Au NPs solution were measured using a KSV 3000 LB trough at room temperature. The results are shown in Figure 1(a), where we can see that the film is fully compressible up to a pressure of 1.09 mN/m. Above this pressure, the film becomes much more difficult to compress, and finally collapses above a pressure of 11.59 mN/m. In order to visualize the internal ordering of the particle films, and determine the mean radius of the particles, films obtained at different pressures were lifted onto Transmission electron microscopy(TEM) grids and imaged. From Figure S1, we can see that at a surface pressure of 2 mN/m, the film still has a empty space, which at 3 mN/m appears to be nearly completely closed. If further pressure is applied the film immediately buckles (Cartoon picture in Figure S1). This isotherms are consistent with previous results reported by Sun *et al.*[26] for Au nanoparticles synthesized in the same manner. From the TEM images we can see that in this case as well, the particles form films with patches where close packed local order is observed among the particles. With increasing pressure, a uniform film is formed with long ranged close packed order, which collapses into multiple, disordered segments at the highest pressure. The particle size was obtained by analyzing the image of the film shown in Figure 2(a), which was lifted off the surface onto a TEM grid at the center of the π-A isotherms, where the incompressible monolayer is formed at a pressure of π = 3 mN/m. The average particle diameter, d = 2.71±0.83 nm, obtained from the histogram shown in Figure 2(b), is consistent with that previously reported by Sun *et al.*[26]. Very long ranged order is observed across the entire image, where the particles are assembled in close packed order, with a spacing of 1.2 nm between the perimeters of the particles which can be obtained from the fast fourier transform(FFT) transform of the image. The crystalline orientation of the particles lifted from the air water interface was further analyzed using high resolution TEM. The image of a typical particle is shown in Figure 3(a), where we can clearly see that the diffracted image corresponds a twinned single crystal where the two facets are joined at 26°. The electron diffraction images are consistent with an FCC orientation with a lattice of a = 4.074 Å, which is the same as that of bulk gold (a=4.0786 Å). EXAFS spectra obtained previously from Au NPs and PdNPs films synthesized by the Brust method and lifted from the air/water interface onto kapton supports, indicated that the particles were not spherical, but rather had a truncated cuboctahedron structure, with a 2:1 aspect ratio and with a thickness was nearly half the particle diameter[26]. In order to determine the thickness of the particles in the films used to coat the Nafion membrane, the films were also lifted onto native oxide covered Si wafers at pressures of 2 mN/m, 3 mN/m and 10 mN/m. The profiles were then measured using X-ray reflectivity and the data together with the fitted curves are shown in Figure 3(f) from which we obtain a thickness of 1.58 nm for the particles in the monolayer film. A partial thiol layer was detected at the particle/air interface, but could not be found at the particle/Si interface. This was consistent with the hydrophilic nature of the film and confirmed that the particles were in direct contact with the substrate surface.

The particle layer formed at this pressure was also lifted onto a Si substrate coated with a 19.7 nm thick layer of Nafion, where the same thickness was ob-

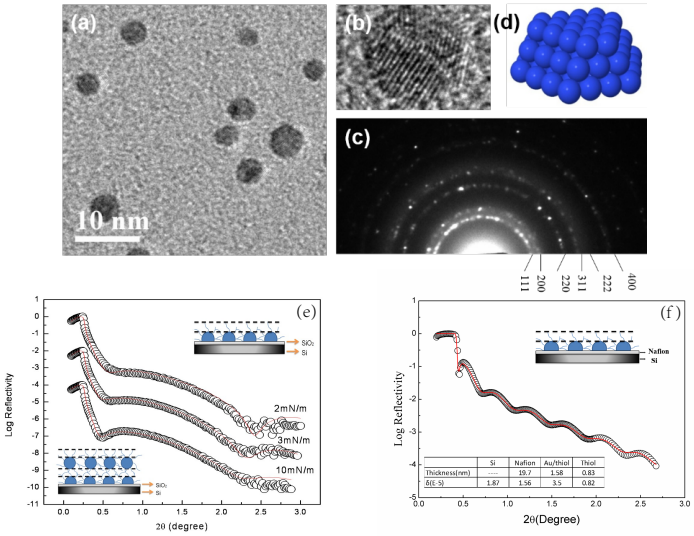

Figure 3: (a) High resolution transmission electron microscopy(HRTEM) image of thiol-stabilized gold nanoparticles (b) magnified image of one nanoparticle (c) electron diffraction of the particle. (d) the cartoon of three atomic layer gold nanopartilces. (e) X-ray reflectivity measurement for the Au NPs on silicon substrate: X-ray reflectivity original curve (circles) and fit curve (red line). Top inset: cartoon illustration of Au NPs monolayer on top of silicon wafer; Bottom inset: cartoon illustration of Au NPs multiple layers on top of silicon wafer. (f) X-ray reflectivity measurement and fitting parameters for the Au NPs on Nafion substrate: X-ray reflectivity original curve (circles) and fit curve (red line). Top inset:cartoon illustration of Au NPs monolayer on top of nafion thin film spun cast on the silicon substrate; Bottom inset: fitting results from reflectivity measurements.

tained(see Figure 3(e) and Table S1), confirming that the oblate particles were formed at the air/water interface, and were not a function of the substrate upon which they were lifted. From the reflectivity measurements we were also able to deduce that the density of the thiol layer at the Si interface was very low, which was consistent with the hydrophilic nature of the film, and the displacement of the Au-thiol. For the collapsed film two layers are observed, the one originally in contact with water surface is 1.74 nm, and a second layer 3.74 nm, or nearly twice the thickness, is formed above it. This indicates that only the layer in contact with the substrate surface is oblate, but as the layer is lifted off the surface recombination of the particles to their spherical shape occurs. A table listing the fitting parameters for the curves is provided in the supplementary materials section.

The X-ray reflectivity results were also confirmed using TEM analysis of the films lifted from the LB trough. The thickness of the particles deduced from EXAFS was in good agreement with that measured from reflectivity. Hence the Au particles lifted onto the Nafion membrane by this procedure offer a good approximation to morphology of the particles proposed by Mavrikakis *et al.*[27]. From the data we can also see that the Au/water interface is highly unstable and when collapsed, the particles recombine to form a layer with the same thickness as the original particles. Hence these particles also had the potential of being highly reactive, and effective at catalyzing, also in agreement with the predictions of Mavrikakis *et al.*[27]

Au NPs were lifted onto Nafion membranes, as shown, were a layer was deposited onto both sides of the membrane. Membranes with and without Au NPs coatings were then inserted into a single stack PEM fuel cell, where the power output could be measured across a variable resistance bridge. The optimum H_2 flow rate, was first determined and found to be 80 ccm (cm^3/min, 25°C, 1 atm), regardless of whether the membranes were coated or uncoated. The polarization curves are plotted in Figure 4(a), where we can see that the curve obtained with the Au NPs coated membrane is significantly higher than the one obtained with the uncoated membrane, when the PEM is run with the cathode open to atmosphere. In Figure 4(b) we plot the maximum power obtained in our test station at a minimum load of 0.5 Ohms where we can see that we obtain a value of 18 mW/cm^2 and 9.52 mW/cm^2 for the coated and uncoated MEAs respectively, which represents an enhancement of 88%. We also experimented with adding the Au NPs directly to the membrane, without liftoff from the air/water interface, or depositing the Au NPs

from the air/water interface directly on the electrodes rather than on the membrane. No enhancement of the power output was observed in either case, indicating that the catalytic process involving the Au NPs required both oblate shaped particles as well as direct surface contact with the Nafion membrane. Figure 1(b) we plot the maximum power output as a function of the pressure with which the Au NPs were lifted from the air/water interface. From the figure we can see that the max power rises linearly with surface pressure, reaching a maximum at 3 mN/m. Hence in this region the power is directly proportional to the number of oblate particles, or the area covered by the particles on the Nafion membrane. Once the film is complete, the maximum surface area is covered, and no additional oblate particles can be introduced. Additional surface pressure, results in buckling of the Au NPs layer already formed, which reduces the effective area covered only by the oblate particles. From the figure we see that the output is continuously reduced with increasing surface pressure, till the initial value is observed again at a surface pressure of 11 mN/m where the X-ray reflectivity results showed that a second layer of spherical particles had formed. The results show that the power is directly proportional to the surface coverage, as long as a monolayer has not formed. Once the monolayer has formed the output decreases in direct proportion to the formation of the second layer, which seems to block the effect produced by the first layer. It has been previously established that Au NPs are very effective at catalyzing the CO oxidization reaction when deposited on metal oxide supports[13]. As was discussed previously CO can form during routine operation under ambient conditions of the PEM fuel cell, where the oxidation of CO can be the rate limiting step. Therefore in order to explain the large enhancement of the power output observed only when

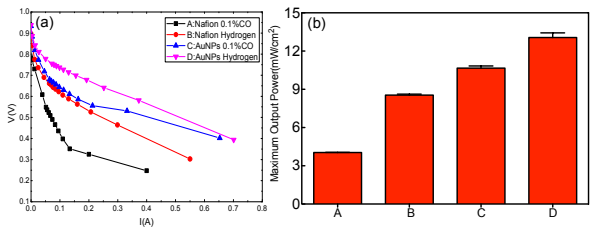

Figure 4: (a) Performance measurement for a single stack under mixure feed gases with 0.1% CO on anode side. (b) Maximum output power density of PEM fuel cell, A: Nafion membrane under mixure feed gases with 0.1% CO; B: Nafion membrane under pure hydrogen gas; C: Au NPs coated Nafion membrane under mixure feed gases with 0.1% CO; D: Au NPs coated Nafion membrane under pure hydrogen gas.

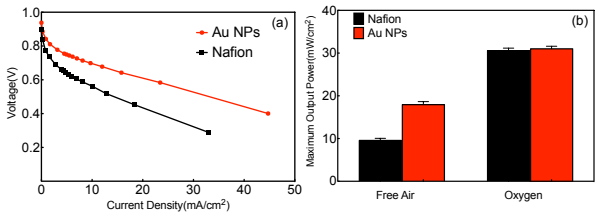

Figure 5: Performance measurement for (a) single stack cell, surface pressure we choose to deposit gold nanoparticles onto Nafion membrane is 3 mN/m (b) Maximum Output Power measured by H-Tec PEMFC kit under different cathode feed gas, air and oxygen separately.

the membrane is coated by the oblate nanoparticle layers, we postulated that the Nafion polymer was somehow acting on the adsorbed reactants in a manner similar to the metal oxide supports which Mavrikakis[27] and Yates[9] had shown to reduce the energy barrier of the oxidation. In order to probe this hypothesis we measured the differential in the power output between coated and uncoated membranes when the PEM fuel cell was operated in air vs pure O_2. The data shown in Figure 4(b) where we can see the presence substitution of air with pure O_2 at the cathode increases the overall efficiency of the fuel cell, but not additional enhancement is obtained by the nanoparticles. In this case, since CO_2 is not present, water is formed when the H^+ ions emerging from the membrane are oxidized directly by the O_2. Hence no advantage is obtained by the presence of the Au NPs or reduction of the barrier to CO oxidation. In contrast, in Figure 5(a) we show the polarization curves when 0.1% CO is mixed with the input H_2 flow to the PEM fuel cell. From the figure we can see that in the absence of Au NPs the output is decreased by 53%, whereas the decrease for the PEM fuel cell with the Au NPs coated membrane the decrease is only 16%, confirming that the oblate Au NPs coating is enabling oxidation of the CO.

In order to determine the applicability of these nanoparticle platelets to high current industrial MEAs, testing is currently underway in collaboration with Fuel Cells Etc., a third party testing laboratory. Preliminary results have been very promising indicating an enhancement of at least 25% (Figure S2).

DFT calculations were carried out to understand the origin of improved output power obtained by direct depositing Au NPs on Nafion membranes. Au NPs with 3-atomic layer in height and 2 nm in size were constructed to model the experimentally synthesized Au NPs generated by spreading thiol-functionalized spherical Au NPs at the air-water interface (Figure 6). The Au-Nafion in-

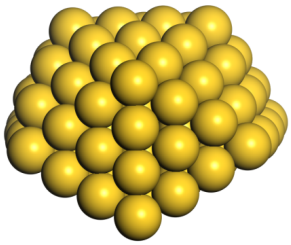

Figure 6: DFT-optimized structure for a 2 nm Au nanoparticle.

teraction was simulated by adsorbing a SO_3-containing group, which is attached at end of Nafion side chains. CO oxidation to CO_2 was studied, assuming that the facile removal of CO in the solution by Au NPs can help to release the CO poisoning on the active Pt sites and therefore increase the overall conversion.

The results show that the SO_3 species provided by Nafion play an essential role, being able to effectively oxidize CO to CO_2 at the perimeter sites of Au NPs and therefore reduce the amount of CO. The SO_3 species are strongly adsorbed at the low-coordinated Au sites via the three terminal oxygen atoms. The barrier (Ea) for oxidizing the adsorbed CO nearby (SO_3 + CO $\rightarrow$ SO_2 + CO_2) is only 0.518 eV (Figure 7(a)). Without SO_3, the removal of CO on the Au NP via the water-gas reaction (WGSR, H_2O +CO$\rightarrow$ CO_2 + H_2) is energetically very difficult on both Au and Pt catalysts, e.g. the highest Ea for the WGSR on a Au NP is 1.292 eV [28, 29]. In our model, the adsorbed SO_3 on Au NP is used as a simplified model to describe the interaction between Au and Nafion membranes. The interaction between SO_3 and Au is rather weak, which results in a facile removal of one of oxygen from SO_3 to oxidize CO with a barrier as low as 0.518 eV. The further weakening is expected if the ligands attached to SO_3 in Nafion are included, Au-SO_3-R. On the contrary, if it is strongly bound on Au, the CO oxidation by SO_3 will be energetically hindered due to its high stability.

According to the calculated barriers, the rate constant for CO oxidation on the Au NP was estimated roughly via $\frac{k_bT}{h}e^{-\frac{E_a}{k_bT}}$. As shown in Figure 7(b), the rate constant decreases depending on the oxidant used, $H_2O \ll SO_3$, which leads to the decreasing of reaction temperature from 539 K to 223 K to achieve a rate constant of 102 $s^{-1}site^{-1}$ for instance. Given that, the direct interaction between Au and nafion membranes is necessary to facilitate the CO oxidation and therefore release the CO poisoning, where Au NPs act as an active oxidation catalyst and the nafion provides the efficient oxidant.

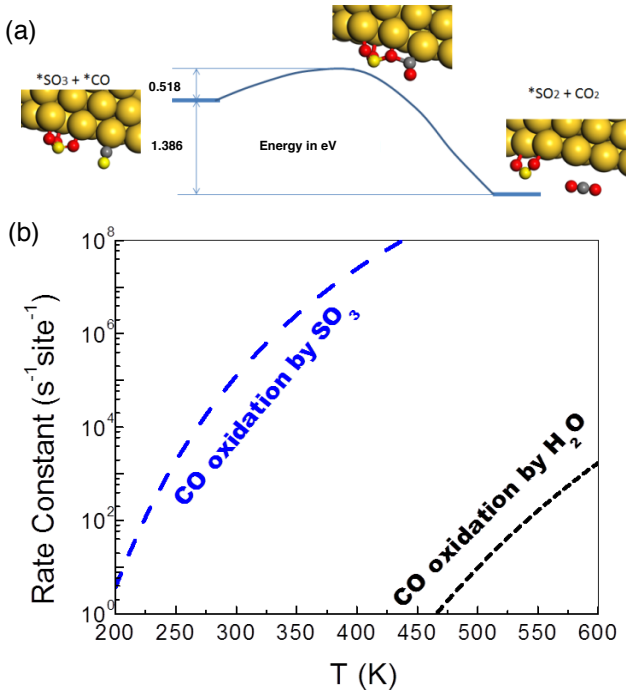

Figure 7: DFT-calculated transition (a) and rate constant as a function of temperature T. (b) for CO oxidation on a Au NP. Big gold: Au; small red: O; small yellow: S; Small grey: C.

4. Conclusions

In conclusion we have shown that combining the Brust method for Au NPs synthesis with LB film technology, it is possible to produce oblate Au NPs .When the Nafion membranes of hydrogen fuel cells are coated with a monolayer of the particles, the power output can be enhanced by more than 50% when the fuel cells are operated under ambient conditions. No enhancement is observed when oxygen is substituted at the cathode and more than 200% when 0.1% CO is added to the hydrogen gas stream at the anode. DFT calculations show that the SO_3 species provided by Nafion play an essential role in reducing the activation barrier for the oxidation of CO to CO_2 at the perimeter sites of Au NPs, enabling the operation of PEM fuel cells with higher power at lower temperatures.

Acknowledgement

Funds for research work at Brookhaven National Laboratory were provided by the U.S. Department of Energy, Office of Basic Energy Sciences, under Contract No. DE-SC-00112704. DFT calculations were

performed using computational resources at the Center for Functional Nanomaterials, a user facility at Brookhaven National Laboratory. The work at Stony Brook University was funded in part by PowerbridgeNY under a NYSERDA29750 grant, and by a grant from SGRID3 of the Long Island Regional Economic Development Council 2014.

References

[1] O. J. Murphy, G. Hitchens, D. J. Manko, Proceedings of the fourth space electrochemical research and technology conference high power density proton-exchange membrane fuel cells, Journal of Power Sources 47 (3) (1994) 353 – 368. doi:http://dx.doi.org/10.1016/0378-7753(94)87014-4.

[2] R. Devanathan, Recent developments in proton exchange membranes for fuel cells, Energy Environ. Sci. 1 (2008) 101–119. doi:10.1039/B808149M.

[3] H. Zhang, P. K. Shen, Recent development of polymer electrolyte membranes for fuel cells, Chemical Reviews 112 (5) (2012) 2780–2832. doi:10.1021/cr200035s.

[4] L. Carrette, K. A. Friedrich, U. Stimming, Fuel cells: Principles, types, fuels, and applications, ChemPhysChem 1 (4) (2000) 162–193. doi:10.1002/1439-7641(20001215)1:4¡162::AID-CPHC162¿3.0.CO;2-Z.

[5] T. V. W. Janssens, B. S. Clausen, B. Hvolbæk, H. Falsig, C. H. Christensen, T. Bligaard, J. K. Nørskov, Insights into the reactivity of supported au nanoparticles: combining theory and experiments, Topics in Catalysis 44 (1) (2007) 15–26. doi:10.1007/s11244-007-0335-3.

[6] J. J. Baschuk, X. Li, Carbon monoxide poisoning of proton exchange membrane fuel cells, International Journal of Energy Research 25 (8) (2001) 695–713. doi:10.1002/er.713.

[7] W.-M. Yan, H.-S. Chu, M.-X. Lu, F.-B. Weng, G.-B. Jung, C.-Y. Lee, Degradation of proton exchange membrane fuel cells due to co and co_2 poisoning, Journal of Power Sources 188 (1) (2009) 141 – 147. doi:http://dx.doi.org/10.1016/j.jpowsour.2008.11.107.

[8] M. Haruta, M. Dat, Advances in the catalysis of au nanoparticles, Applied Catalysis A: General 222 (12) (2001) 427 – 437. doi:http://dx.doi.org/10.1016/S0926-860X(01)00847-X.

[9] I. X. Green, W. Tang, M. Neurock, J. T. Yates, Spectroscopic observation of dual catalytic sites during oxidation of co on a au/tio_2catalyst, Science 333 (6043) (2011) 736–739. doi:10.1126/science.1207272.

[10] S. Minicò, S. Scirè, C. Crisafulli, A. Visco, S. Galvagno, Ft-ir study of au/fe_2o_3 catalysts for co oxidation at low temperature, Catalysis Letters 47 (3) (1997) 273–276. doi:10.1023/A:1019081727173.

[11] M. M. Schubert, S. Hackenberg, A. C. van Veen, M. Muhler, V. Plzak, R. Behm, Co oxidation over supported gold catalystsinert and active support materials and their role for the oxygen supply during reaction, Journal of Catalysis 197 (1) (2001) 113 – 122. doi:http://dx.doi.org/10.1006/jcat.2000.3069.

[12] E. D. Park, J. S. Lee, Effects of pretreatment conditions on co oxidation over supported au catalysts, Journal of Catalysis 186 (1) (1999) 1 – 11. doi:http://dx.doi.org/10.1006/jcat.1999.2531.

[13] M. Haruta, Gold as a novel catalyst in the 21st century: Preparation, working mechanism and applications, Gold Bulletin 37 (1) 27–36. doi:10.1007/BF03215514.

[14] M. C. Kung, R. J. Davis, H. H. Kung, Understanding au-catalyzed low-temperature co oxidation, The Journal of Physical Chemistry C 111 (32) (2007) 11767–11775. doi:10.1021/jp072102i.

[15] M. Haruta, N. Yamada, T. Kobayashi, S. Iijima, Gold catalysts prepared by coprecipitation for low-temperature oxidation of hydrogen and of carbon monoxide, Journal of Catalysis 115 (2) (1989) 301 – 309. doi:http://dx.doi.org/10.1016/0021-9517(89)90034-1.

[16] I. X. Green, W. Tang, M. McEntee, M. Neurock, J. John T. Yates, Inhibition at perimeter sites of au/tio_2 oxidation catalyst by reactant oxygen, Journal of the American Chemical Society 134 (30) (2012) 12717–12723. doi:10.1021/ja304426b.

[17] N. Lopez, J. K. Nørskov, Catalytic co oxidation by a gold nanoparticle: a density functional study, Journal of the American Chemical Society 124 (38) (2002) 11262–11263. doi:10.1021/ja026998a.

[18] M. Okumura, S. Nakamura, S. Tsubota, T. Nakamura, M. Azuma, M. Haruta, Chemical vapor deposition of gold on al_2o_3, sio_2, and tio_2 for the oxidation of co and of h2, Catalysis Letters 51 (1) 53–58. doi:10.1023/A:1019020614336.

[19] J.-D. Grunwaldt, C. Kiener, C. Wgerbauer, A. Baiker, Preparation of supported gold catalysts for low-temperature cooxidation via size-controlled gold colloids, Journal of Catalysis 181 (2) (1999) 223 – 232. doi:http://dx.doi.org/10.1006/jcat.1998.2298.

[20] Y. Sun, A. I. Frenkel, R. Isseroff, C. Shonbrun, M. Forman, . Kwanwoo Shin, T. Koga, H. White, L. Zhang, Y. Zhu, M. H. Rafailovich, , J. C. Sokolov, Characterization of palladium nanoparticles by using x-ray reflectivity, exafs, and electron microscopy, Langmuir 22 (2) (2006) 807–816. doi:10.1021/la052686k.

[21] B. Delley, From molecules to solids with the $dmol^3$ approach, The Journal of Chemical Physics 113 (18) (2000) 7756–7764. doi:http://dx.doi.org/10.1063/1.1316015.

[22] B. Delley, An allelectron numerical method for solving the local density functional for polyatomic molecules, The Journal of Chemical Physics 92 (1) (1990) 508–517. doi:http://dx.doi.org/10.1063/1.458452.

[23] J. P. Perdew, J. A. Chevary, S. H. Vosko, K. A. Jackson, M. R. Pederson, D. J. Singh, C. Fiolhais, Atoms, molecules, solids, and surfaces: Applications of the generalized gradient approximation for exchange and correlation, Phys. Rev. B 46 (1992) 6671–6687. doi:10.1103/PhysRevB.46.6671.

[24] T. A. Halgren, W. N. Lipscomb, The synchronous-transit method for determining reaction pathways and locating molecular transition states, Chemical Physics Letters 49 (2) (1977) 225 – 232. doi:http://dx.doi.org/10.1016/0009-2614(77)80574-5.

[25] M. Brust, M. Walker, D. Bethell, D. J. Schiffrin, R. Whyman, Synthesis of thiol-derivatised gold nanoparticles in a two-phase liquid-liquid system, J. Chem. Soc., Chem. Commun. (1994) 801–802doi:10.1039/C39940000801.

[26] Y. Sun, A. I. Frenkel, H. White, L. Zhang, Y. Zhu, H. Xu, J. C. Yang, T. Koga, V. Zaitsev, M. H. Rafailovich, , J. C. Sokolov, Comparison of decanethiolate gold nanoparticles synthesized by one-phase and two-phase methods, The Journal of Physical Chemistry B 110 (46) (2006) 23022–23030. doi:10.1021/jp060432h.

[27] M. Mavrikakis, P. Stoltze, J. Nørskov, Making gold less noble, Catalysis Letters 64 (2) (2000) 101–106. doi:10.1023/A:1019028229377.

[28] P. Liu, J. A. Rodriguez, Water-gas-shift reaction on metal nanoparticles and surfaces, The Journal of Chemical Physics 126 (16) (2007) 164705. doi:http://dx.doi.org/10.1063/1.2722747.

[29] L. C. Grabow, A. A. Gokhale, S. T. Evans, J. A. Dumesic, , M. Mavrikakis, Mechanism of the water gas shift reaction on pt: first principles, experiments, and microkinetic modeling, The

Journal of Physical Chemistry C 112 (12) (2008) 4608–4617.
doi:10.1021/jp7099702.